SEDIMENTATION IN SUBMERGED SINKHOLES IN FILLMAN'S CREEK, A MICROTIDAL ESTUARY IN WESTERN FLORIDA, USA

A Thesis

by

JAKE AUSTIN EMMERT

Submitted to the Office of Graduate and Professional Studies of
Texas A&M University
in partial fulfillment of the requirements for the degree of

MASTER OF MARINE RESOURCES MANAGEMENT

Chair of Committee,	Peter J. van Hengstum
Co-Chair of Committee,	Samuel Brody
Committee Member,	Timothy Dellapenna
Head of Department,	Patrick Louchouarn

August 2016

Major Subject: Marine Resources Management

ABSTRACT

Sediment archives in sinkholes and blueholes in both Cenozoic and Mesozoic carbonate platforms preserve important records of paleoenvironmental change. However, there is still a poor understanding of detailed sedimentary mechanisms operating in these systems in western Florida. Fillman's Creek is a microtidal estuary in western Florida that contains two sub-tidal sinkholes, with an urbanized watershed around its periphery. Given the close proximity (~500 m) of the two sinkholes, Huck's Hole (HCK) and Sawyer's Sink (SYR), one would expect coherent sedimentation patterns at each site (e.g., texture, structure, and inputs). However, the two sinkholes have different sedimentation patterns and sedimentation rates, which indicate different processes likely control sedimentation in these two sites.

The different sedimentary constituents at each site dictated that different methods of textural analysis were used for each site (e.g., laser particle size analysis, classic loss on ignition). Chronological control was established with radiocarbon dating and ^{137}Cs activity in the sediment cores. Organic matter particles and lenticular and horizontal sand deposits dominate the stratigraphy in HCK, and a 6 m sediment core spans 1942 CE to present. These sediment patterns indicate (i) a high sedimentation rate, (ii) the preferential trapping of mangrove-derived particles in the downstream sinkhole site, and (iii) that multiple hydrodynamic processes are driving sand deposition into HCK (e.g., tides and storms). In contrast, sedimentation in SYR is dominated by fine-grained

siliclastic and organic sediment particles that are interrupted with visually-distinct coarse-grained horizons.

Problematically, suitable age control for the successions from Sawyer's Basin is hampered by a lack of terrestrial plant macrofossils, but available radiocarbon ages (on bivalves) and ^{137}Cs data do suggest a change in sedimentation rate in Sawyer's Basin sometime in the last several hundred years. A lack of suitable age control and low sedimentation rates precludes a confident association of coarse-grained horizons to possible hurricane layers in Sawyer's Basin. Given the significant sedimentary differences observed in the sinkholes from the same microtidal estuary, these results indicate the complexity of sedimentation in sinkholes on Florida's western coast.

ACKNOWLEDGEMENTS

I would like to thank my advisor, Dr. P. van Hengstum, and the members of my thesis committee, Dr. S. Brody and Dr. T. Dellapenna, for their guidance and support throughout the course of this research and my time at Texas A&M University at Galveston. Thanks also go to my friends and colleagues and the department faculty and staff for making my time at Texas A&M University a remarkable experience. I also want to extend my gratitude to the Coastal Geoscience Group, which provided survey instruments and lab equipment, to the Laboratory for Oceanographic and Environmental Research, which provided lab equipment and guidance, and the Center for Texas Beaches and Shores, which provided lab equipment and guidance.

The recovery and analysis of the Fillman's Creek sediment cores was supported by a Texas Institute of Oceanography Graduate Summer Fellowship, the Erma Lee and Luke Mooney Travel Grant, and an NSF research grant to PvH. Key logistical and other support was provided by Meghan Horgan, Paul Laverty, Josh Williams, Matt Athon, Chen Xu, Helen Walters and Jacque Cresswell.

Finally, thanks to my mother and father for their encouragement and love.

TABLE OF CONTENTS

Page

ABSTRACT ii

ACKNOWLEDGEMENTS iv

TABLE OF CONTENTS v

LIST OF FIGURES vii

LIST OF TABLES viii

1. INTRODUCTION 1

1.1 Research questions and hypotheses 3

2. SEDIMENTATION PATTERNS IN SINKHOLES AND BLUEHOLES 5

2.1 Sedimentation in offshore sinkholes and blueholes 5
2.2 Sedimentation in terrestrial sinkholes, blueholes, and cenotes 6
2.3 Sedimentation in inland Floridian sinkholes and caves 8
2.4 Sedimentary processes in microtidal estuaries 9

3. REGIONAL SETTING 12

4. METHODS 16

4.1 Fieldwork 16
4.2 Sedimentary analyses 16
4.3 Geochronology 18

5. RESULTS 20

5.1 Hydrography 20
5.2 Sediments in HCK-D2 21
5.3 Sediments in SYR 24
5.4 Chronology and sedimentation rates 27

6. DISCUSSION 31

6.1 What are the differences and drivers of sedimentation and sedimentation rates in the Fillman's Creek sinkholes? 31

6.2 How has proximity to mangroves influenced sedimentation in the two sinkholes?....34
6.3 Are hurricane signals archived as coarse-grained overwash deposits into the sinkhole, and does the stratigraphic record preserve a record of hurricane activity?....35
6.4 Has coastal urbanization impacted sedimentation rates in the sinkholes?....37

7. CONCLUSIONS....40

REFERENCES....42

LIST OF FIGURES

Page

Figure 1. Fillman's Creek is located in western Florida, USA (A), and the microtidal estuary has 2 sinkholes (B,C). 13

Figure 2. Historic anthropogenic modification around Fillman's Creek. Fillman's Creek in 1941 CE (A), in 1974 CE (B), in 2013 CE (C), and Fillman's Creek within subimage C (D). 14

Figure 3. Profiles of the coastal aquifer at Fillman's Creek. Blue and orange distinguish the hydrographs of SYR and HCK, respectively. 20

Figure 4. Photographs depicting examples of organic material and distinct sand layers observed in HCK core. (A) mangrove propagule and shell fragment; (B) marine bivalve interbedded in organic rich siliciclastic matrix consistent throughout core; (C) sand layer at 340.5 cm; (D) salient coarse horizon from 450.5 to 465.5 cm with gravel-sized sediment particles. 22

Figure 5. Huck's Hole sedimentary diagram. Sand layers (i.e., lenticular and storm layers) and diverse organic matter can be seen in the lithology. The ^{137}Cs outlier at approximately 450 cm is reworked material deposited with the salient coarse layer. The radiocarbon date at 180 cm is likely from old, reworked sedimentary material. 23

Figure 6. SYR-D4 sedimentary characteristics. Distinct sand layers and shell fragments are visible within the finely-laminated (~1 mm laminations) siliciclastic matrix. 25

Figure 7. Sedimentary characteristics of SYR-D1, SYR-D3, and SYR-D4. PSDs are indicated by volume for each core. Mean and D90 analyses are shown for each core. SYR-D3 shows the sieve first method and classic LOI (%OM) results. Radiocarbon results for SYR-D1 and SYR-D3 are shown in Cal years BP, and are 2σ values. 26

Figure 8. HCK age model and linear interpolated sedimentation rates. A distinct change in sedimentation rate occurs at 1995 CE (inflection point; see discussion). Age at base of core (~1941 CE) was determined by linear extrapolation using preceding sedimentation rate. 30

LIST OF TABLES

Page

Table 1. Radiocarbon results from SYR and HCK. All possible 1σ and 2σ calibrations and their probabilities are provided below, but only the highest 2σ calibration result was incorporated into their respective age models. Index point number 2 was too old for inclusion into the age model. 28

1. INTRODUCTION

Continuing research over the past three decades has significantly increased our understanding of sinkhole and bluehole sedimentology, and the value of their sediments to understanding millennial-scale paleoenvironmental change. For example, sedimentary accumulations in sinkholes and blueholes archive: decadal and millennial scale patterns in late Holocene hurricane activity (Denommee et al., 2014; Lane et al., 2011; van Hengstum et al., 2016; van Hengstum et al., 2013), glacioeustatic sea-level change and subsequent paleohydrographic development (Kovacs et al., 2013; van Hengstum et al., 2010; van Hengstum et al., 2011; Zarikian et al., 2005), and even evidence of terrestrial climate variability (Grimm et al., 1993). However, the specific drivers of sedimentation in North American sinkholes and blueholes is still emerging (Collins et al., 2015a; Collins et al., 2015b; van Hengstum et al., 2010; van Hengstum et al., 2011).

Sinkholes and blueholes are abundant karst features on Mesozoic (e.g., Little Bahama Bank, Great Bahama Bank) and Cenozoic (e.g. Florida Peninsula, USA) carbonate platforms in the North Atlantic region (Budd, 2001; Jansa, 1981). It is worth noting that the terms bluehole, sinkhole, and cenote are derived from their prominent regional usage in the Bahamas, Florida, and Yucatan Peninsula, respectively. In fact, the term ‘bluehole’ is not frequently applied in the Florida region, yet submerged, offshore sinkholes are known from western Florida (Culter, 2006; Garman and Garey, 2005; Swarzenski et al., 2001), southern Florida (Land and Paull, 2000), and eastern Florida (Shinn et al., 1996). Although blueholes and sinkholes typically form by subsurface

carbonate dissolution followed by collapse of the overlying carbonate (Mylroie et al., 1995; Mylroie et al., 1995b; Mylroie, 2013), the specific geomorphologic origin of these features is geographically variable. For example, some Floridian sinkholes are connected to the cave systems, which are thought to have formed by subsurface dissolution during lower paleo water levels (Brinkmann and Reeder, 1994; Florea, 2006; Gulley et al., 2013; Gulley et al., 2014; Mylroie and Mylroie, 2013). Other systems have a notably structural origin, such as the circle of cenotes in the Yucatan Peninsula from the Terminal Cretaceous Chixulub impact event. Once formed, however, sinkholes and blueholes offer a natural sediment trap to isolate sediments from many post-depositional processes (e.g., particle redistribution in the surf zone).

Most investigations on sinkhole sediments in the North Atlantic region remain focused in the Caribbean region or inland Florida, with little information available for coastal sinkholes in western Florida, USA. In general, sedimentation in offshore Caribbean blueholes is dominated by carbonate sedimentation (Denommee et al., 2014; Gischler et al., 2008; van Hengstum et al., 2013), with organic matter and carbonate materials from both terrestrial and aquatic sources dominating sediment sources in terrestrial sinkholes. Deposition of siliciclastic sedimentary particles is notably diminutive in the Caribbean area; however, inland Floridian systems can accumulate significant quantities of siliciclastic sedimentary particles, in addition to terrestrial and aquatic organics and carbonate particles that can be either inorganically or biologically sources. For example, hurricane events in Apalachicola Bay deposited siliciclastic sand particles into Mullet Pond, a sinkhole basin in northwestern Florida (Lane et al., 2011).

More work is needed to better understand the overarching and site-specific processes influencing sedimentation in Florida's sinkholes.

1.1 Research questions and hypotheses

Fillman's Creek is a microtidal estuary on the western coast of Florida that contains two sinkholes separated by 500 m: Huck's Hole and Sawyer's Basin (see section 2.0). Huck's Hole is located ~600 m from the mouth of the estuarine entrance, and Sawyer's Basin is located further upstream. This site geometry allows for an investigation into the sedimentary processes impacting two submerged sinkholes on the western coast of Florida. Long-term coastal urbanization in the adjacent watershed may have further impacted sinkhole sedimentation during the historic interval. While regional sediment transport and depositional processes of coastal microtidal estuaries, such as Fillman's Creek, are present in the literature, the depositional processes of the sinkholes within these systems have been overlooked. Using Fillman's Creek as a research site I plan to answer three questions, and test their associated hypotheses:

(1) What are the primary sedimentary constituents and sedimentation rates in submerged sinkholes in Fillman's Creek? I hypothesize that the sinkhole closest to the estuary mouth with more mangrove trees will have higher organic matter deposition and sedimentation rates.

(2) Have the sinkhole sedimentation rates changed in response to land cover modification of the adjacent watershed? I hypothesize that landscape change

from coastal development has increased the sedimentation rates of local estuaries by altering local sediment delivery pathways to coastal systems.

(3) Do the sinkholes record long-term hurricane activity on the western coast of Florida through deposition of overwash layers? I hypothesize that hurricanes will promote deposition of coarse-grained overwash deposits into the sinkhole, which will preserve a record long-term of hurricane activity in the stratigraphic record.

2. SEDIMENTATION PATTERNS IN SINKHOLES AND BLUEHOLES

2.1 Sedimentation in offshore sinkholes and blueholes

Sedimentation in offshore (submerged by sea level) Caribbean blueholes appears dominated by alternating fine- and coarse-grained carbonate sedimentary layers denoting fair-weather and storm conditions, respectively. For example, Great Blue Hole on Lighthouse Reef in Belize (80 km offshore, ~120 m depth) has a sedimentation rate of 2.5 mm yr^{-1}, with alternations between fine (mean grain size 10 to 30 µm) and coarse grained layers (>30 µm) (Denommee et al., 2014). Elsewhere, Thatchpoint Blue Hole (69.2 m depth) on the Little Bahama Bank, is dominated by fine-grained carbonate mud with a mean grain size between 15 and 25 µm and has a sedimentation rate of ~ 1.75 cm yr^{-1} (van Hengstum et al., 2013). Peaks of coarse sand (>8%) and coarse silt (>22%) layers are present, with a mean 8.8% fine-grained bulk organic matter (OM) (van Hengstum et al., 2013). In Florida, a 600 m diameter offshore bluehole (5.7 m water depth) on the Florida reef tract is rapidly infilling with aragonitic mud, perhaps up to 54.5 m depth (Shinn et al., 1996). Shinn et al. (1996) and others suggest that during sea-level lowstands, freshwater (or stratified coastal groundwater) would have flooded the karst basin, and deposition transitioned to aragonitic mud sedimentation after the basin was inundated by Holocene sea-level rise.

The factors governing sedimentation in offshore sinkholes appears to be local sediment supply (i.e., marine sands transported from the surrounding shallow shelf, van Hengstum et al. 2013), biological processes (algal precipitation, carbonate skeleton

production), inorganic carbonate precipitation (Gischler and Zingeler, 2002; van Hengstum et al., 2013) and a combination of fair-weather infilling and tropical cyclone strikes (Gischler et al., 2008). The dominance of carbonate sediment in these settings is unsurprising, given that these systems lie within the carbonate factory.

2.2 Sedimentation in terrestrial sinkholes, blueholes, and cenotes

Caribbean tropical and subtropical forests often surround sinkholes on the terrestrial landscape, and these basins often host aquatic ecosystems since they are flooded by the local coastal aquifer (Schmitter-Soto et al., 2002). As such, these systems receive both terrestrial (forest litter) and aquatic (algae) organic matter inputs and both biologic (shells) and inorganic carbonate particles (calcite mud). The relative contribution of these sedimentary constituents to the stratigraphic record can vary on millennial timescales, as changes in groundwater level and hydrographic conditions can alter the background environmental conditions within the sinkhole itself (Teeter and Quick, 1990). For example, Runway Sinkhole (~225 m inland, 1.8 m depth), on the coast of Great Abaco Island in the Bahamas accumulated a peat deposit >4000 years ago, which indicates that sedimentation was then dominated by organic matter. However, these peat deposits pass into carbonate sediments upsection as concomitant Holocene sea-level and groundwater-level rise shifted the environment into an aquatic anchialine ecosystem ~1200 years ago (Kovacs et al. 2013). In contrast, sedimentation has been negligible in Laguna Chumkopo (10 km inland, 80 m depth) on the Yucatan Peninsula in Mexico since the middle Holocene (~7000 years ago), but hurricane events

deposited fining upward sequences in the sinkhole when storms elevate lagoonal hydrodynamics, re-mobilize and re-deposit middle Holocene sediments into the deep, shaft-style sinkhole. As a result, Chumkopo sinkhole has alternating fine-grained (coarse silt to clay) and coarse-grained carbonate (sand, mean 355 μm) deposition. Cenote Yax Chen (~300 m inland, ~10 m depth) is a sinkhole surrounded by a mangrove swamp that gives access to the inland Yax Chen Cave system on the coast of the Yucatan Peninsula, Mexico, which is part of the much larger Ox Bel Ha Cave System. Collins et al. (2015b) describe sedimentation in Yax Chen Cave as dominated by mangrove sedimentary products in cave passages that are proximal to the cenote, which provides amorphous fine-grained flocs of organic matter for deposition into the adjacent cave system (range ~ 40 to 43% OM). In the Bahamas (Andros Island), Church's Blue Hole is a terrestrial basin that is 33 m deep and ~ 5 km inland, and sedimentation includes units dominated by shells and algal gyttja, shells and calcareous mud, calcareous mud and finely laminated algal gyttja (Kjellmark, 1996). It is likely that the sedimentation is documenting changing hydrographic conditions within the sinkhole itself, perhaps from local precipitation and groundwater changes over the late Holocene (Kjellmark, 1996). Also in the Bahamas, Emerald Pond (Abaco Island) is a terrestrial basin located ~2.4 km inland with a 2.6 m water depth, where sedimentation has varied between carbonate mud, macrofossils and varying inputs of organic matter over the last ~8000 years (2 to 85% OM) (Slayton, 2010). Although this is not an exhaustive review of Caribbean sinkholes and their known sedimentary processes, it emphasizes the complexity of sinkhole sedimentary processes and the need for continuing sedimentological research in

these systems to resolve their relationships between primary sedimentary layers and specific environmental processes.

2.3 Sedimentation in inland Floridian sinkholes and caves

In contrast to the sinkholes elsewhere in the tropical Atlantic, Floridian systems receive siliciclastic sediment input in addition to carbonates and organic matter. For example, Lake Tulane is ~107 km inland from the Gulf of Mexico, has a water depth of 22.7 m and its sediments contain little carbonate constituents (Grimm et al., 1993). Camel lake in northwest Florida is also a sinkhole basin that is located ~54 km inland. Camel lake has modern deposition of black gyttja, with basal orange-hued peats and alternating layers of peaty silt or silt with some sand (Watts et al., 1992). The sediments in Little Salt Spring, an inland Florida sinkhole, consists of a basal 1.2 m thick quartz-rich sand deposit, followed by 9.8 m of laminated and unconsolidated detrital organic material and carbonate-rich sediments. Coarse layers were noted within the 12,000-year archive, however, a paleohydrologic reconstruction of the Floridian aquifer was the primary objective of the study. Little Salt Spring is ~19 km from the coast and has a water depth of 72 m (Zarikian et al., 2005).

In northwestern Florida, sedimentation in Mullet Pond (~400 m inland, ~2.3 m depth) is characterized by a basal freshwater peat deposit that passes into gyttja with varying amounts of quartz sand input from hurricane overwash events. The stratigraphy within Mullet Pond produced a 4500-year record of hurricane activity from the coarse-grained siliciclastic layers deposited by elevated hydrodynamics from hurricane events

(Lane et al., 2011). Elsewhere in western Florida, Hole in the Wall Cave and Twin Cave in Marianna, Florida contain ferromanganese deposits (Winkler et al., 2016). Indeed these results indicate that these systems can record paleohurricane activity, potential evidence for groundwater-level changes, and subsequent hydrologic development our understanding of the drivers of modern sedimentation in these systems remains incomplete.

2.4 Sedimentary processes in microtidal estuaries

Physical and biological processes in nearly all estuaries are influenced by tides (Wells, 1995). Tidal influence in large Gulf of Mexico estuaries (i.e., San Antonio Bay, Corpus Christi Bay, Galveston Bay, and Mobile Bay) is diminished by the small tidal range around the Gulf (>1 m for all them) (Davis Jr and Fitzgerald, 2009). Traditionally, runoff from rivers encounters tidal flux, and this interaction is the primary driver of siliciclastic sedimentation in estuaries from both landward and seaward locations (Davis Jr and Fitzgerald, 2009). In contrast, some microtidal estuaries along Florida's western coast are generated by fresh groundwater from subterranean karst conduits or matrix porosity. This groundwater directly mixes with the ocean in the coastal zone in the absence of surface rivers, and they have recently been referred to as *karst estuaries* (Menning et al., 2015). A key difference between these two estuarine settings in the Gulf of Mexico are differences of annual sediment load transported by annual inflow. The Vermillion/Atchafalaya Bay System is a traditional river-supplied estuary with the largest annual sediment load in the northern Gulf of Mexico (37.5 million tons per year).

In contrast, Tampa Bay is a karst estuary in Florida that has some additional river input and it carries the lowest annual sediment load (0.21 millions of tons per year) (Isphording et al., 1989).

The drivers of sedimentation in karst estuaries (i.e., west-central Florida) are interpreted as a result of low sediment supply, storms and tidal currents, bathymetry, and related antecedent topography (i.e., shallow bathymetry and sinkholes) (Brooks and Doyle, 1998). Both Tampa Bay and Charlotte Harbor receive sediments from peninsular Pleistocene terrace deposits, and freshwater inputs can create predominant terrigenous clastic mud facies (Brooks and Doyle, 1998).

Both natural and anthropogenic factors impact sedimentation in microtidal environments. The limited tidal energy can govern, or limit, the amount of inorganic sediment input (Stevenson et al., 1986), however, sedimentation from hurricanes or extra-tropical low-pressure systems can be a critical factor reorganizing sediments (Baumann et al., 1984; Reed, 1989; Rejmanek et al., 1988). Schoellhamer (1995) observed winter storm and tropical storm generated wind waves as a primary natural sediment resuspension mechanism at two sites (4 m and 1.5 m depth) in Old Tampa Bay, Florida, with little resuspension of upper bay silts and sands from tidal currents.

Land use change in coastal watersheds is known to impact sedimentation in adjacent coastal environments. In siliciclastic systems, land-use change from a natural to an urbanized environment generally increases sediment delivery to coastal environments through subaerial drainage networks (Lee et al., 2006). Additionally, urbanization is a major cause of loss of coastal wetlands, and exerts significant influences on the structure

and function of these systems mainly through modification of hydrological and sedimentation regimes (Lee et al., 2006). Increased surface runoff from impervious surfaces combined with disturbed soils can accelerate the scouring of sediments and the resultant transport and deposition in receiving wetlands (Horner, 2000). Urbanized watersheds can mobilize sediment through altered hydrographic pathways, and runoff is the main sediment transport path, including eroded soil from construction sites (Horner, 2000). Watershed issues and sediment dynamics studied in the Tijuana River National Estuarine Research Reserve found watershed urbanization, along with local climate, topography, and soils, has resulted in extreme rates of sedimentation accumulation (e.g., 10 to 30 cm over a single winter in 1994 to 1995). These observations exceeded historic sedimentation rates in the estuary or rates from other coastal wetlands with storm sedimentation (Callaway and Zedler, 2004).

3. REGIONAL SETTING

Fillman's Creek is located on the western coast of Florida (USA) near New Port Richey (north of Tampa) (Fig 1). This area is part of the karst region known as the Ocala Karst Plain, which is ~600 m of varying Eocene, Oligocene and Pleistocene eogenetic reefal limestone (Florea et al., 2009; Puri, 1957; Randazzo et al., 1990; Scott and Anderson, 2001).

Fillman's Creek is currently a shallow estuary (mean water depth <1 m) with a mean tidal range of 0.7 m (microtidal) (NOAA, 2015). The Pithlachascotee (~5 km north) and Anclote (~ 7 km south) rivers constrain Fillman's Creek estuary. This estuary contains small tidal creeks and extensive mangroves around the periphery, but mangroves are especially concentrated around the mouth of the system. The northwestern versus southeastern portions of the estuary are separated by a road, but these sections remain hydrographically connected by a culvert. In addition to the road, the watershed surrounding Fillman's Creek has experienced progressive coastal urbanization throughout the 20th century. Abundant sinkholes and tidal creeks are present on the surrounding coastal landscape prior to 1941 CE (Fig. 2A), but a residential community and road network are present in the area by 1974 CE (Fig. 2B). The culvert dividing Fillman's estuary was installed by 1957 CE (Figs. 2C, 2D) (Aerial Park Survey, 1974; Surveys, 1957). Based on the Gulf of Mexico sea-level curve from Milliken et al. (2008), sea level was −10 to −3 m below present from 8000 to 4000 years

ago. Therefore, Fillman's Creek and its sinkholes were progressively inundated by regional base-level rise from Holocene sea-level rise during the last several millennia.

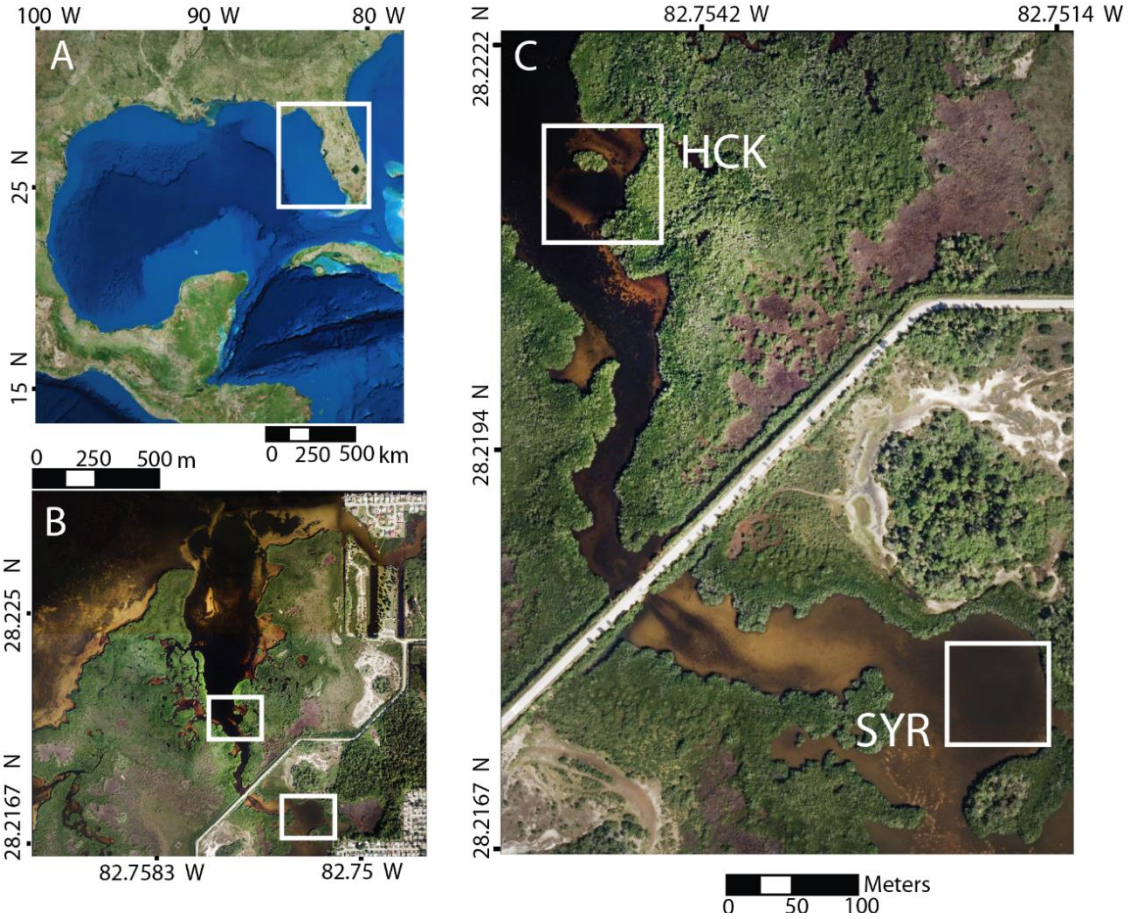

Figure 1. Fillman's Creek is located in western Florida, USA (A), and the microtidal estuary has 2 sinkholes (B,C).

Two sinkholes are present in Fillman's Creek, Huck's Hole (28.221°N, 82.754°W), and Sawyer's Basin (28.217°N, 82.751°W) (Fig. 1). Huck's Hole (HCK) is located ~650 m from the mouth of the estuary, it is surrounded by mangroves along its

east and west edges, and the depth to the sediment-water interface is 11.3 m. In contrast, Sawyer's Basin is located 1.26 km from the estuary entrance and is separated from HCK by the culverted road crossing, and mangroves are on the banks of the basin. Depth to the sediment-water interface is centered in Sawyer's Basin and is 5.9 m.

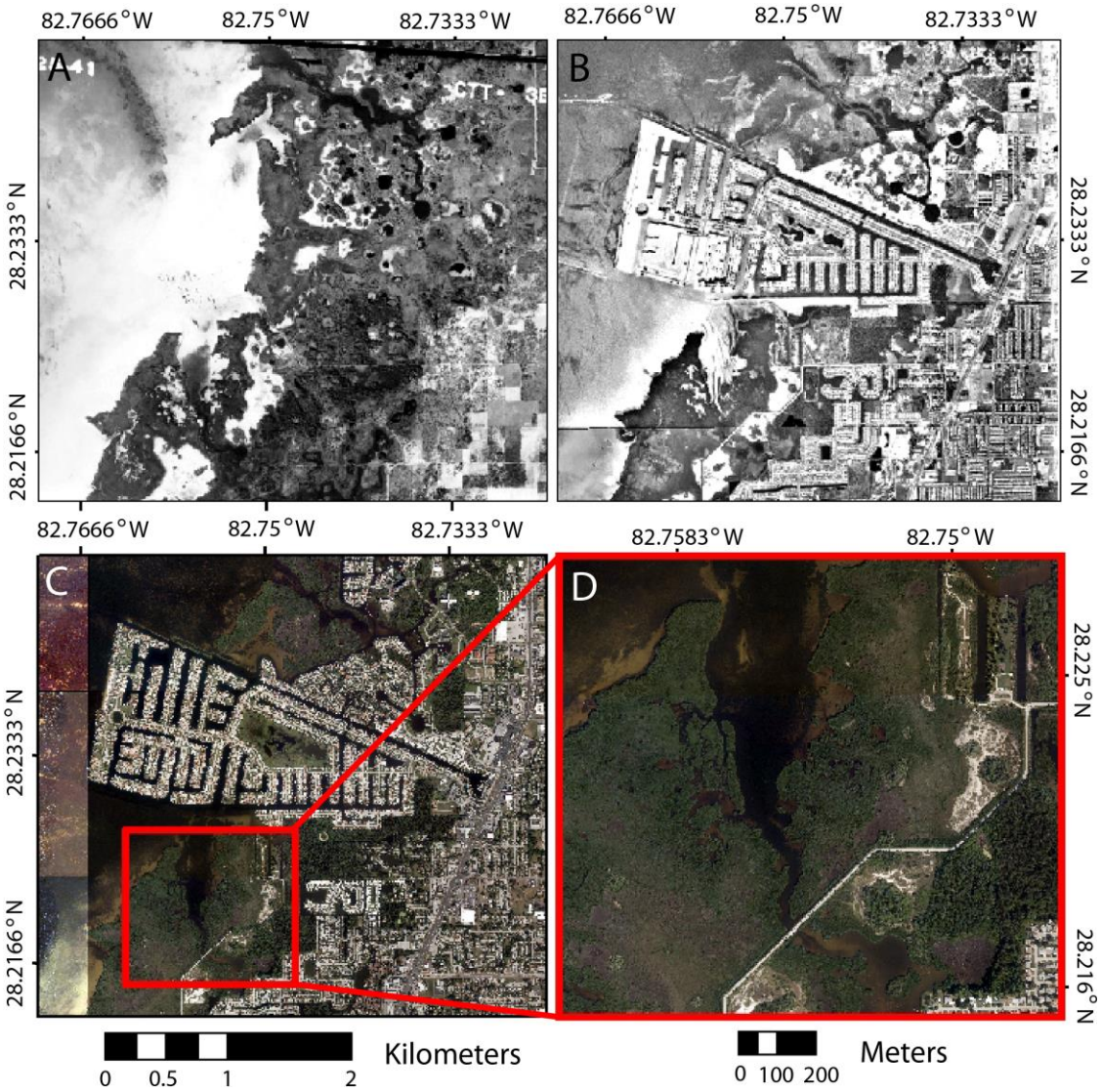

Figure 2. Historic anthropogenic modification around Fillman's Creek. Fillman's Creek in 1941 CE (A), in 1974 CE (B), in 2013 CE (C), and Fillman's Creek within subimage C (D).

Based on the National Oceanic and Atmospheric Administration's HURDat database of historic hurricanes, a total of 38 storms made landfall or crossed within 75 km of Fillman's Creek since 1850 CE. Of these storms, only 4 were classified as intense hurricane events (exceeding category 3 on the Saffir-Simpson scale): (1) an unnamed hurricane struck as a category 3 in October of 1921; (2) an unnamed hurricane crossed the radius as a weakening category 4 in September of 1935; (3) an unnamed hurricane struck as a weakening category 3 in August of 1949; and (4) Hurricane Easy struck as a category 3 in September of 1950.

4. METHODS

4.1 Fieldwork

Vibracores were collected from the sinkholes in Fillman's Creek in 2011 and 2012. A vibracore (HCK-D2) was collected from Huck's Hole using a Rossfelder P3 on the *R/V Arenaria* (Woods Hole Oceanographic Institution). The total recovered length of HCK-D2 was 614 cm. For Sawyer's Basin, 7.6 cm diameter rod-driven vibracores were collected from a raft (total lengths: SYR-D1 179 cm, SYR-D3 142 cm, SYR-D4 198 cm). After collection cores were transported back in the laboratory where they were sectioned lengthwise, X-radiographed to image internal sedimentary structures, and stored at 4°C until further analysis. Hydrographic parameters in the sinkholes were measured on 6 September 2014 with a YSI EXO1 multiparameter sonde, which was calibrated with reference pH and conductivity solutions before deployment. Parameters measured, with uncertainties, were conductivity (±0.001 mS/cm), depth (±0.004 m), dissolved oxygen (±0.1 mg/L), pH (±0.1 pH units), temperature (±0.01°C), and salinity (±0.1 psu).

4.2 Sedimentary analyses

The methods for textural analysis of the sediment from each sinkhole was determined by the different sedimentary constituents at each site. In short (see Results for details), Sawyer's Basin was dominated by fine-grained sediment (SYR-D1, SYR-D3, and SYR-D4), whereas Huck's Hole was dominated by coarse-grained organic

matter particles (core: HCK-D2). Sediment cores from Sawyer's Basin (SYR-D1, SYR-D3, and SYR-D4) were contiguously sampled downcore at 5 mm intervals, and particle size was measured with a Malvern Mastersizer 2000 laser particle size analyzer, which measures individual particle diameters from 0.02 to 2000 μm with a precision of < 2 μm. Resultant particle size distributions (PSDs) were plotted as a color surface plot using MATLAB (sedi3D script), with no interpretation algorithm, to allow comprehensive visualization of sediment texture (Beierle et al., 2002). To isolate variability in just the sand-sized siliciclastic fraction, a suite of sediment samples were also subjected to a Sieve-First Loss-on-Ignition procedure (van Hengstum et al., 2016). A known sediment sample (2.5 ml) was first sieved over a 63 μm mesh to retain coarse particulates. Samples were then dried overnight at 80°C, weighed, combusted at 550°C for 4.5 hours, and re-weighed to determine contribution of sand-sized siliciclastic fraction to the sedimentary matrix. The coarse fraction data represents the mass of sedimentary particles, per cubic centimeter of sediment that exceeds a diameter of 63 μm ($D_{>63\ \mu m}$ mg cm^{-3}).

In contrast, HCK-D2 was dominated by organic matter, so textural variability was examined through a classic loss on ignition (LOI) procedure followed by sieving. This was performed on 1 cm intervals down core of HCK to determine weight-percent (wt %) of organic matter content and sand content (>63 μm sized particles). First, sediment samples were dried overnight at 80°C, weighed, combusted at 550°C for 4.5 hours, and re-weighed to determine relative contribution of organic matter to the sedimentary dry mass (Heiri et al., 2001). After combustion, remaining ash and

inorganic sediment were wet sieved over >63 μm mesh to retain coarse sand fractions, dried overnight at 80°C and reweighed to calculate weight percent sand relative to original sample.

4.3 Geochronology

Chronological control was established with radiocarbon dating and ^{137}Cs activity in the sediment cores. The samples were aged using traditional AMS measurements from the National Ocean Sciences AMS Facility at Woods Hole Oceanographic Institution and International Chemical Analysis Inc. (Miami, Florida). Samples submitted for radiocarbon dating from HCK-D2 included a leaf, a bivalve shell, 2 bulk organic matter samples and 3 twig samples. Samples from SYR included 3 bivalve shells. Once extracted from the respective core, each sample was washed and briefly ultrasonically cleaned to remove adhering contaminant sediment particles, and dried overnight at 80°C and weighed to ensure sufficient sample size for ^{14}C measurement. Conventional radiocarbon ages from HCK were calibrated using the INTCAL13 radiocarbon age calibration curve from Reimer et al. (2013). Unfortunately, there was little ability to control for hardwater effect on the marine bivalves from SYR. Ages with a fraction modern value ($F^{14}C$) exceeding 1.0000 were calibrated with CALIbomb (Hogg et al., 2013; Reimer et al., 2013) using the compiled North Hemisphere Zone 2 dataset (Hua et al., 2013), because we assume these samples were alive post-1950 AD. Conventional radiocarbon ages from SYR were calibrated using the INTCAL13 radiocarbon age calibration curve from Reimer et al. (2013).

To add support to the radiocarbon chronology, ^{137}Cs activity in the sediment was used to further establish chronologic control of the historic period in SYR and HCK. ^{137}Cs is a man-made radionuclide that is able to identify the initiation (~1954 AD) and moratorium (~1963 AD) on nuclear weapons testing based on ^{137}Cs activity in bulk sediment (Pennington et al., 1973; Ritchie and McHenry, 1990). ^{137}Cs and was measured on desiccated and powdered bulk sediment samples from 1-cm intervals in a Canberra Germanium gamma well detector (661 KeV peak for ^{137}Cs). ^{137}Cs samples were dried in an oven over night at 80°C and homogenized with mortar and pestle. Once homogenized, 5 mL of the sample sediment was placed in 10 mL tubes that were placed in a gamma counter well. Sampling time of the gamma counter was 48 hours for each sediment sample.

5. RESULTS

5.1 Hydrography

Two distinct water masses are identifiable in the upper most part of the local coastal aquifer at Fillman's Creek, assuming the hydrographic profile on the day of measurement represents average water quality conditions at the sites. Each site is generally characterized by an upper tidally-mixed, brackish layer above anoxic saline groundwater with a transitional zone from 2 to 3 m below the water surface (Fig. 3).

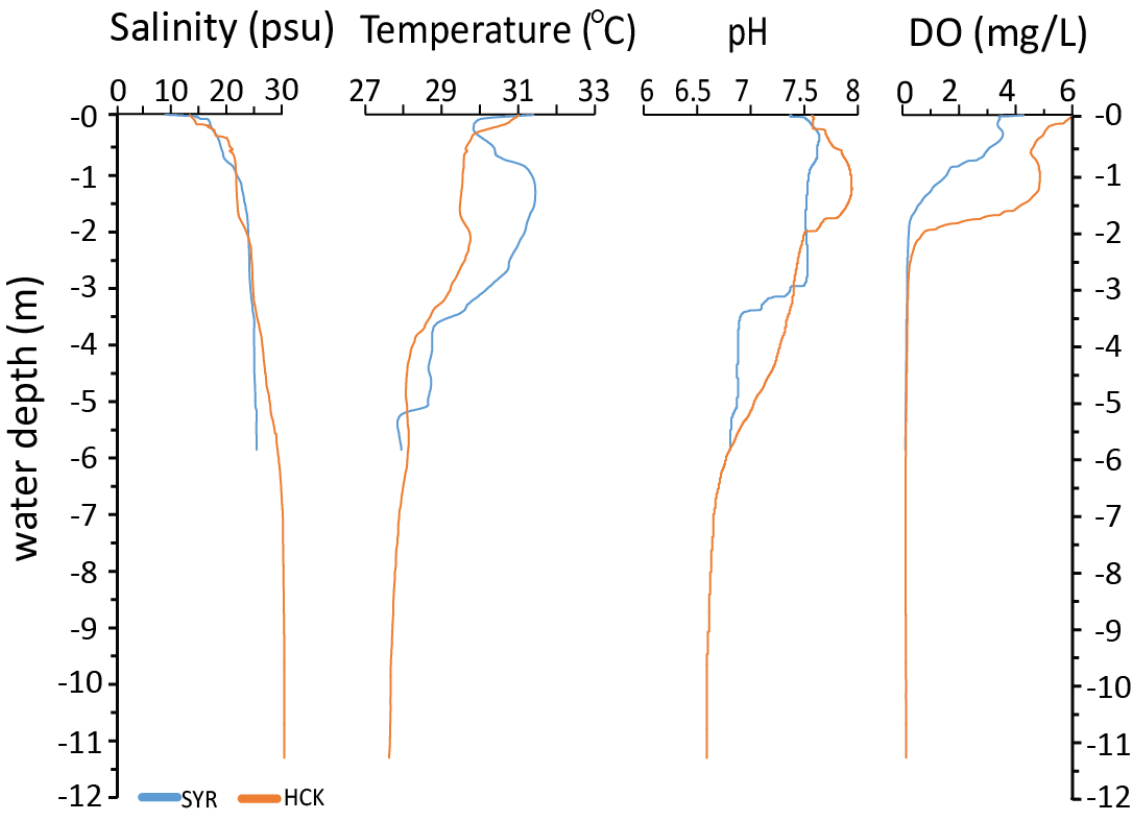

Figure 3. Profiles of the coastal aquifer at Fillman's Creek. Blue and orange distinguish the hydrographs of SYR and HCK, respectively.

The tidally mixed, brackish upper layer is distinguished by salinity, dissolved oxygen, and pH profiles. Surface salinity (~13 psu HCK, ~ 9 psu SYR) sharply increases to 23 psu at 2 m in both sinkholes. From the surface to ~2 m, DO profiles decrease (6 to 0.8 mg l^{-1} HCK, 4.2 to 0.2 mg l^{-1} SYR). Average temperature of the upper water mass is slightly warmer (30°C HCK, 30°C SYR) than the marine groundwater (28°C HCK, 29°C SYR), and decreases in a stepped trend. Below 2 m, salinity gradually increases in the upper part of the coastal aquifer through the anoxic marine groundwater (<0.74 mg l^{-1} HCK, <0.22 mg l^{-1} SYR) to 30 psu and 25 psu, and continues to the sediment-water interface at ~11 m and ~6 m in HCK and SYR, respectively. The pH profiles below 2 m in HCK and 3 m in SYR steadily decrease through the marine groundwater (pH 6.6 to 6.8 both sites) to the sediment-water interface.

5.2 Sediments in HCK-D2

The sediment in HCK-D2 was entirely unconsolidated, organic-dominated material with both lenticular and horizontally continuous sand layers (Fig. 4). Some of the organic matter was identifiable biological debris (e.g., mangrove propagules and leaves) with the majority being undifferentiated fine-grained particles (Fig. 4). Some shell material was also present (e.g., gastropod shells, and marine mollusk: *Melongena corona*). Lenticular sand deposits were observed throughout the core (e.g., 180 cm, 290 cm, 326 cm, 335 cm, 348 cm, 357 cm, 399 cm, 406 cm, 588 cm, 559 cm, and 564 cm), but the most striking stratigraphic feature is a salient coarse layer of sand and carbonate

gravel particles from 450 to 465.5 cm (Fig. 4D). The core contained a mean 52.8% sand (>63 µm), and ranged in sand content from 0.8% to 90.3%. The core contained a mean

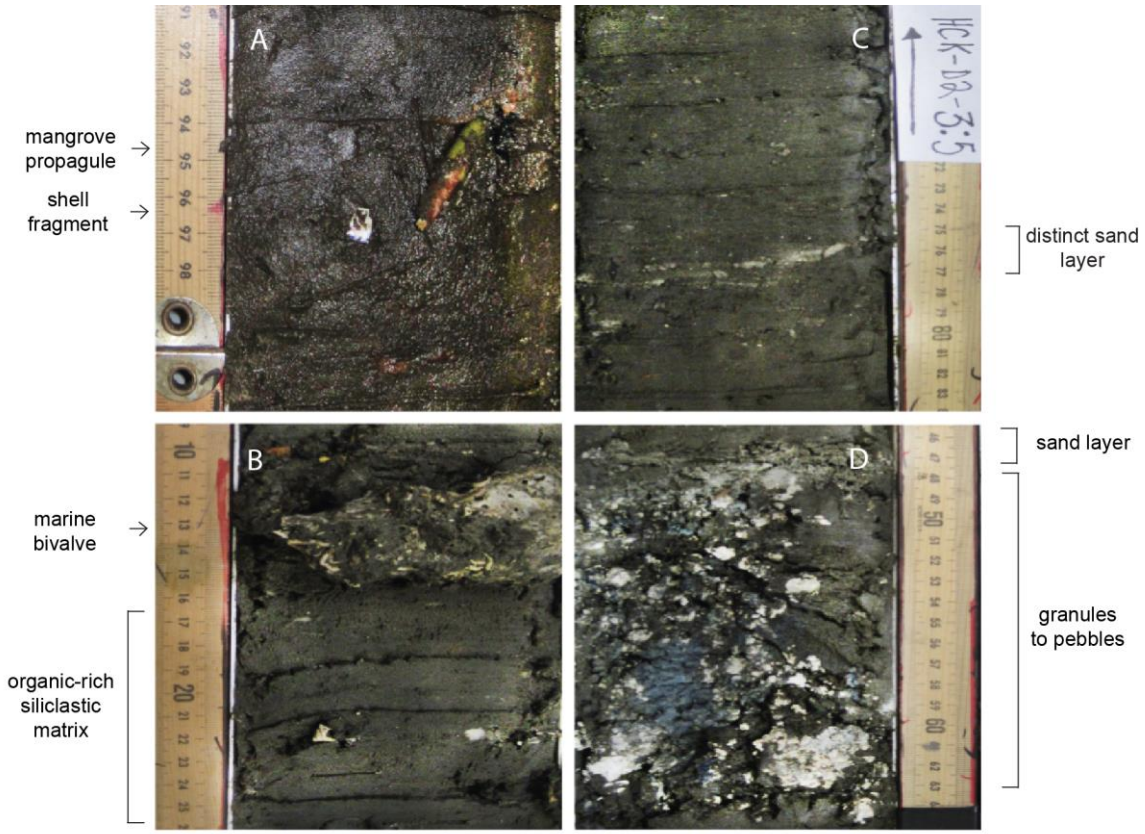

Figure 4. Photographs depicting examples of organic material and distinct sand layers observed in HCK core. (A) mangrove propagule and shell fragment; (B) marine bivalve interbedded in organic rich siliciclastic matrix consistent throughout core; (C) sand layer at 340.5 cm; (D) salient coarse horizon from 450.5 to 465.5 cm with gravel-sized sediment particles.

14.4% bulk organic matter, ranging from 3.7% to 34.6% (Fig. 5). During the LOI procedure, it was notable that after the ignition phase at 550°C, the remaining

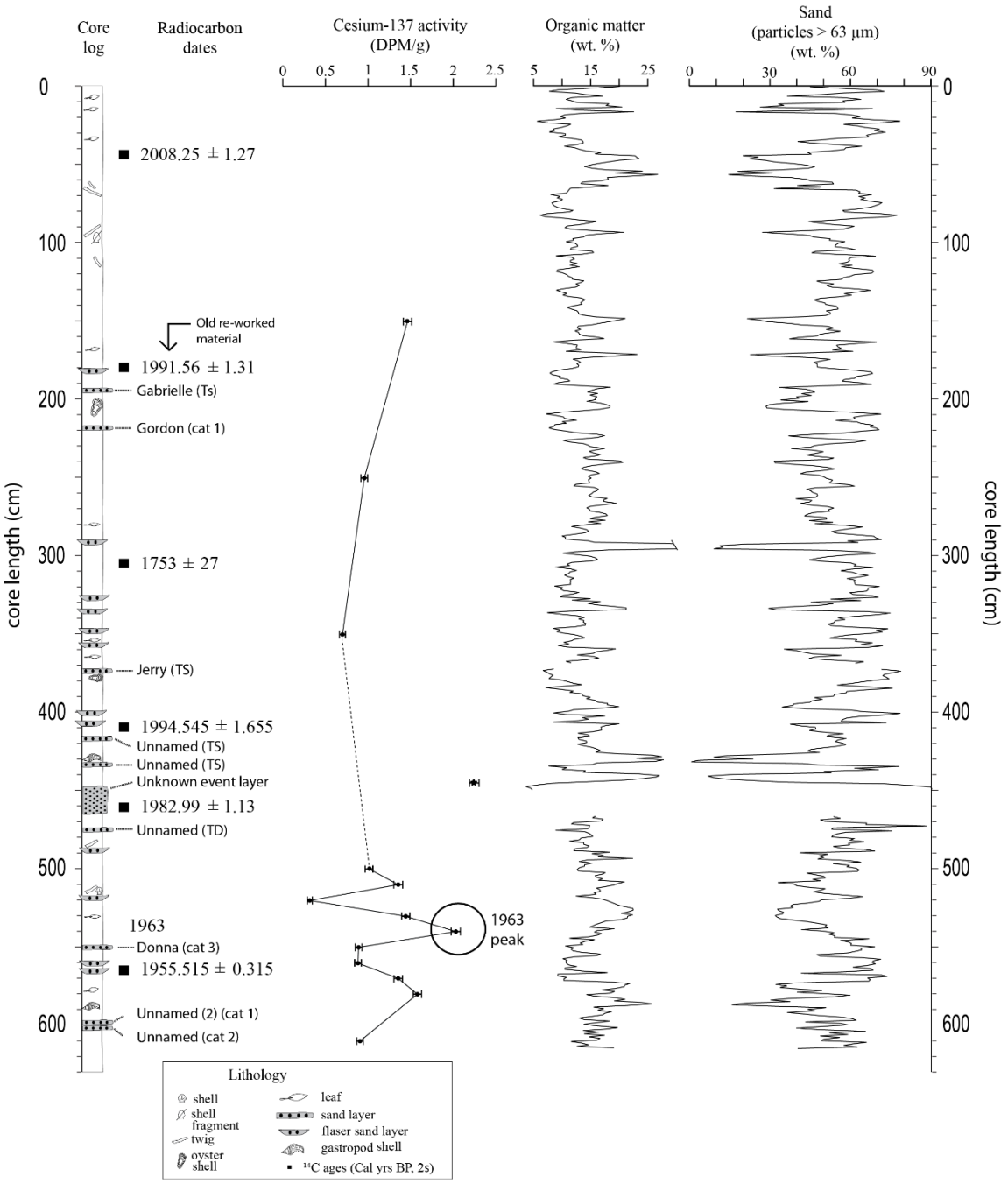

Figure 5. Huck's Hole sedimentary diagram. Sand layers (i.e., lenticular and storm layers) and diverse organic matter can be seen in the lithology. The ^{137}Cs outlier at approximately 450 cm is reworked material deposited with the salient coarse layer. The radiocarbon date at 180 cm is likely from old, reworked sedimentary material.

sedimentary residue had an orange hue, and was significantly consolidated. This may suggest elevated dissolved iron content in the original pore water.

5.3 Sediments in SYR

The texture of sediment in Sawyer's Basin was completely different than in Huck's Hole, which is noteworthy given the close proximity of the two sites. In Sawyer's Basin, sedimentation was dominated by laminated, fine-grained, siliciclastic sediment with interspaced siliciclastic sand layers that were continuous across the core (Fig 6.). The lenticular sand lenses present in HCK-D2 were not present in the cores from Sawyer's Basin. Bulk organic matter was generally indistinguishable from the siliciclastic mud matrix. In general, there is also a notable fining upward trend at the base of the cores SYR-D1 and SYR-D4 at ~150 cm and ~170 cm, respectively. Below this level, texture was slightly coarser in the cores than above, suggesting a subtle change in depositional regime. Detailed textural data for each core from Sawyer's Basin is described below.

SYR-D1 contains laminated siliciclastic sediment with distinct sand layers. The distinct sand layers (e.g. 52 cm, 65 cm, 114 cm, and 121 cm) are also identifiable in the color surface plots of the particle size distributions (Fig. 7). Based on laser particle size analysis, mean particle size was 42.1 μm (medium silt), with a range of 26.8 to 100.8 μm (medium silt to very fine sand). The fining upward sequence captures a mean particle size transition from 59.0 μm to 38.9 μm at 150 cm (Fig. 6). In contrast to the mean grain size metric and PSDs, in which total sediment distributions to include organic matter, the

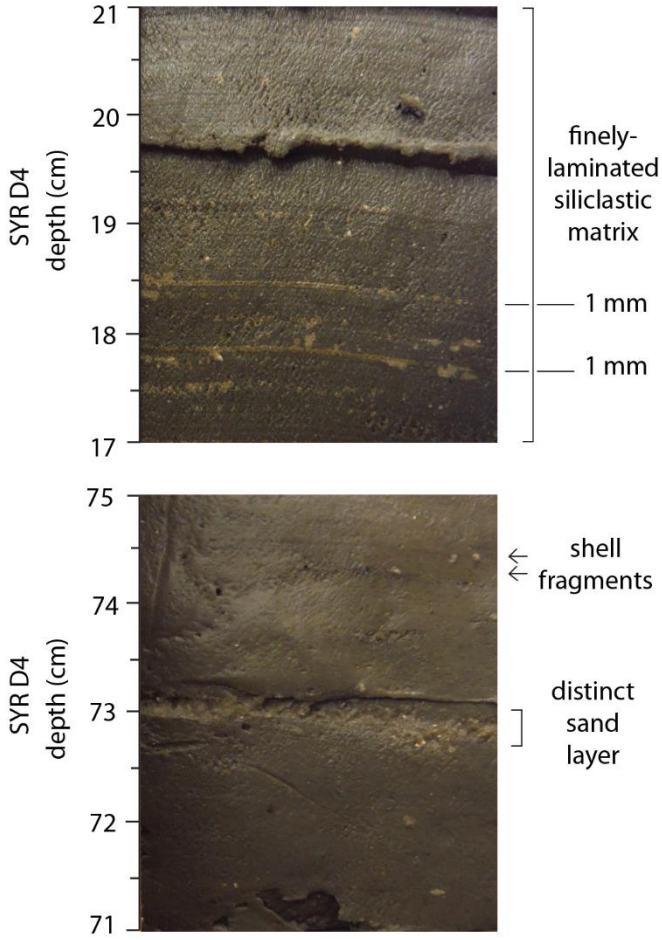

Figure 6. SYR-D4 sedimentary characteristics. Distinct sand layers and shell fragments are visible within the finely-laminated (~1 mm laminations) siliciclastic matrix.

sieving procedure developed by van Hengstum et al. (2013) targets downcore variation in the coarse sand (> 63 μm) fractions, independent of organic matter. The mean of the sieve-first method was 86.2 mg cm^{-3} with a range of 21.6 to 288.7 mg cm^{-3} of the sedimentary particles exceeding the sand-sized range of the Wentworth Scale.

The stratigraphy of SYR-D3 is also laminated, siliciclastic mud with visually distinct sand layers. The distinct sand layers are also identifiable the color surface plots

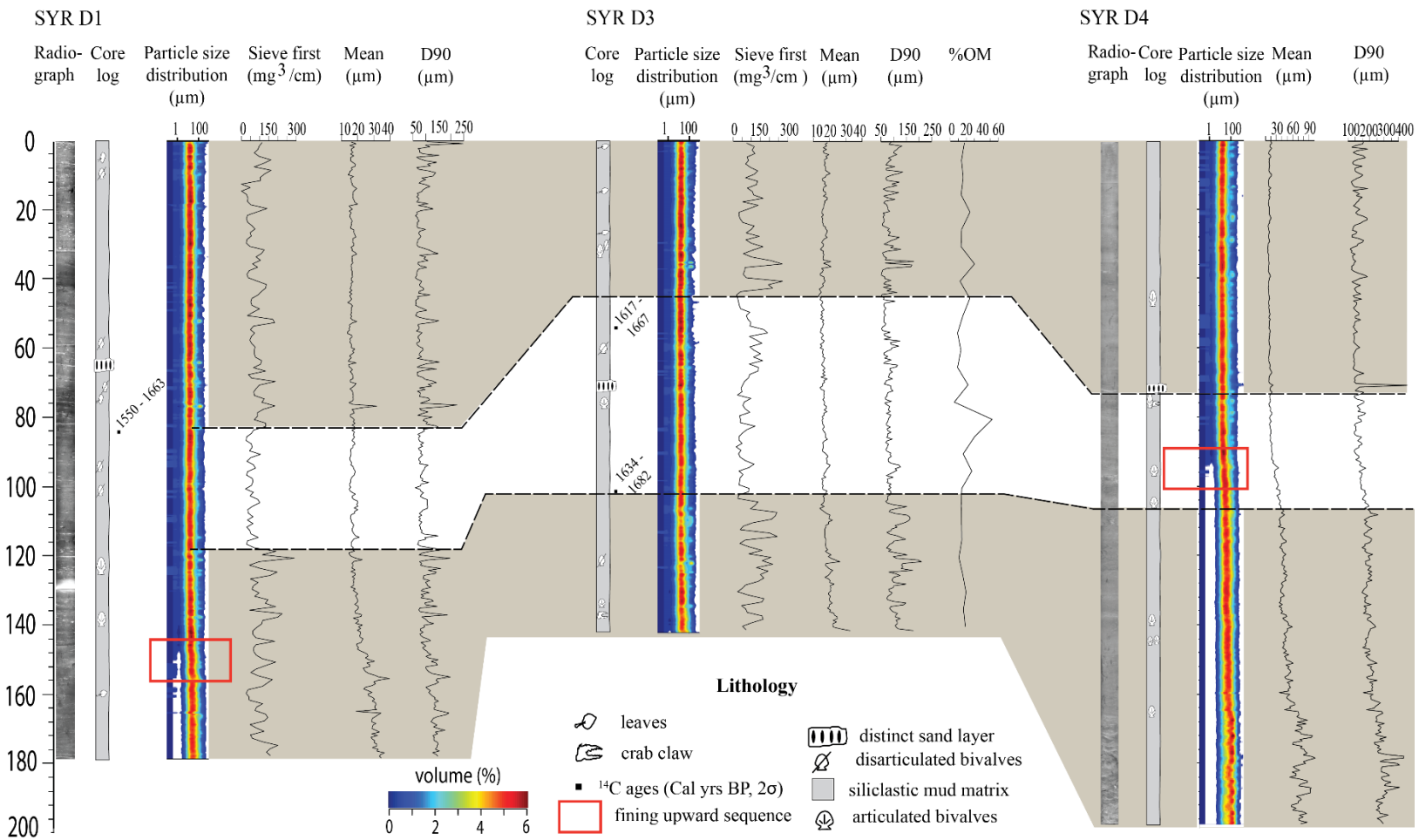

Figure 7. Sedimentary characteristics of SYR-D1, SYR-D3, and SYR-D4. PSDs are indicated by volume for each core. Mean and D90 analyses are shown for each core. SYR-D3 shows the sieve first method and classic LOI (%OM) results. Radiocarbon results for SYR-D1 and SYR-D3 are shown in Cal years BP, and are 2σ values.

of the particle size distributions with a marked shift to a higher volume of coarser sediment (Fig. 7). Based on laser particle size analysis, the mean particle size was 38.5 µm and ranged from 24.4 to 93.9 µm (medium silt to very fine sand). Organic matter content in SYR-D3 based on the classic LOI procedure estimates a mean 17.9% OM by weight, and ranges from 5.0% to 52.3%. The mean of the sieve-first method was 97.3 mg cm^3 with a range of 16.5 to 271.0 mg cm^{-3}. In contrast, HCK-D2 had a mean OM content of 14.4%.

The stratigraphy of SYR-D4 is visually laminated siliciclastic sediment with distinct sand layers (Fig. 6) that are also observed in the PSDs color surface plots. Basedon laser particle size analysis, mean particle size was 70.7 µm and ranged from 28.8 to 177.8 µm (medium silt to fine sand). The fining upward sequence captures a mean particle size transition of 92.3 µm to 44.7 µm at approximately 90 cm (Fig. 7).

5.4 Chronology and sedimentation rates

The radiocarbon and ^{137}Cs results indicate that the entirety of HCK-D2 accumulated in the last 60 years. All radiocarbon dates from HCK-D2 (Table 1) contain more ^{14}C than the modern reference standard, which indicates that the material dated was alive after nuclear weapons testing in the 1950s. This result is also confirmed by the ^{137}Cs activity downcore. The highest probability 2σ calibration result on the ^{14}C age nearest the base of HCK-D2 (566 cm) is March 1955 to October 1955 CE (1955.2 to 1955.83 CE, Table 1). The peak in ^{137}Cs activity (2.03 dpm/g^{-1}) occurs just above this position at 540.5 cm in the core, which represents the 1963 CE chronohorizon associated

Table 1. Radiocarbon results from SYR and HCK. All possible 1σ and 2σ calibrations and their probabilities are provided below, but only the highest 2σ calibration result was incorporated into their respective age models. Index point number 2 was too old for inclusion into the age model.

Index No.	Lab number	Core	Core depth (cm)	Material dated	Fraction Modern ($F^{14}C$)	Conventional ^{14}C age	$\delta^{13}C$ (‰)	2σ calendar ages in yrs. BP (probability)	1σ calendar ages in yrs. BP (probability)
1	OS-112150	HUCKD2	44 to 45	Plant/Wood	1.0536±0.0025		-30.99	1956.63-1957.29 (0.171) 2006.14-2006.32 (0.019) **2006.98-2009.52 (0.810)**	1956.8-1957.07 (0.138) 2007.39-2007.47 (0.037) 2007.83-2009.52 (0.825)
2	14O/1204	HUCKD2	180.5	Bulk Organic Matter	0.9806±0.005		-23.8	1663-1711 (0.184) **1716-1829 (0.473)** 1830-1890 (0.191) 1909-1944 (0.153)	1667-1695 (0.188) 1726-1781 (0.402) 1796-1813 (0.115) 1837-1842 (0.026) 1852-1867 (0.078) 1874-1875 (0.005) 1917-1944 (0.186)
3	OS-115025	HUCKD2	316	Plant/Wood	1.1473±0.0022		-29.95	1958.18-1958.81 (0.066) **1990.25-1992.87 (0.934)**	1990.87-1992.03 (0.972) 1992.60-1992.66 (0.028)
4	14P/1203	HUCKD2	407.5 to 408.5	Plant	1.127±0.005		-19.5	1957.91-1958.65 (0.065) 1992.05-1992.39 (0.032) **1992.89-1996.2 (0.903)**	1993.13-1995.54 (1)
5	OS-112149	HUCKD2	461	Plant/Wood	1.2392±0.003		-27.29	1959.35-1960.92 (0.295) 1961.55-1961.77 (0.065) 1981.01-1981.04 (0.002) **1981.86-1984.12 (0.630)** 1984.90-1984.99 (0.008)	1959.46-1959.86 (0.181) 1961.58-1961.71 (0.076) 1982.14-1983.77 (0.743)
6	OS-112148	HUCKD2	566	Sediment Organic Carbon	1.0069±0.0022		-22.5	**1955.2-1955.83 (1)**	1955.37-1955.69 (1)
7	OS-115077	SYRD1	90.5	Mollusc	0.95736±0.00238	350±20	N/A	1462-1528 (0.446) 1544-1545 (0.002) **1550-1633 (0.552)**	1485-1521 (0.443) 1574-1604 (0.328) 1605-1625 (0.229)
8	15S/0490	SYRD3	54.75	Shell	0.96694±0.0036	270±30	N/A	1515-1597 (0.449) **1617-1667 (0.493)** 1781-1796 (0.057)	1525-1556 (0.404) 1632-1662 (0.596)
9	15S/0491	SYRD3	101.25	Shell	0.97177±0.00362	230±30	N/A	1529-1538 (0.010) **1634-1682 (0.514)** 1735-1804 (0.443) 1935-1944 (0.033)	1645-1669 (0.593) 1780-1797 (0.407)

with the global moratorium on nuclear weapons testing (Pennington et al., 1973). Indeed, there is a marked increase in ^{137}Cs activity at 445.5 cm (to 2.25 dpm /g^{-1}), but this is likely from reworked sediment with high ^{137}Cs activity deposited into HCK after the episodic event that deposited the salient gravel and sand layer at 450 to 465.5 cm. All ages after the basal radiocarbon age align chronologically and add support of continual

deposition. The ages at 461 cm, 408 cm and 44.5 cm are November 1981 to February 1984 CE, November 1992 to March 1996 CE, and December 2006 to July 2009 CE, respectively. The date at 180.5 (Index number 2, Table 1), was too old and was excluded potentially due to a hardwater effect on the bulk organic matter.

In HCK-D2, there is a distinct change in sedimentation rate at 1995 CE (Fig. 8). Sedimentation rates were estimated using linear interpolation between radiocarbon results. The sedimentation rate prior to 1995 CE was 3.34 to 3.75 cm yr^{-1}, but abruptly increases to 26 cm yr^{-1} until 2008 CE where the sedimentation rate slightly decelerates to 16 cm yr^{-1}. The older radiocarbon date at 180.5 cm, likely reworked material, was not included in the estimates of sedimentation rate or age modeling.

Establishing chronological control for the successions from Sawyer's Basin was hampered by a lack of suitable terrestrial plant remains or macrofossils preserved in the recovered cores. However, the ^{137}Cs activity and ^{14}C results from SYR-D1 suggest that sedimentation rates have decreased in Sawyer's Basin at some point in the past. Based on the ^{137}Cs measurements in SYR-D1, the peak in ^{137}Cs activity occurs at a depth of 2.5 cm in the core (i.e., the 1963 CE chronohorizon), which suggests a sedimentation rate in Sawyer's Basin of over ~0.5 mm yr^{-1} over the last ~50 years. Problematically, a bivalve shell from 90.5 cm deep in SYR-D1 was aged to 1590 ± 40 CE. If sedimentation rates were consistently 0.5 mm yr^{-1}, as suggested by the ^{137}Cs activity, then the bivalve at 90.5 cm should have aged to ~201 CE. Indeed, neither a marine reservoir nor a hardwater effect from the antecedent landscape was considered when calibrating the conventional radiocarbon dates until present. However, if applied, these correction

factors would make the resultant calibrated radiocarbon ages for a shell at 90.5 cm even younger. Similarly, the radiocarbon dates on bivalve remains from SYR-D3 at 54.75 and 101.25 cm were 1650 ± 15 CE and 1657 ± 12 CE, respectively. These two dates suggest that sedimentation was previously higher in Sawyer's Basin relative to the most recent past.

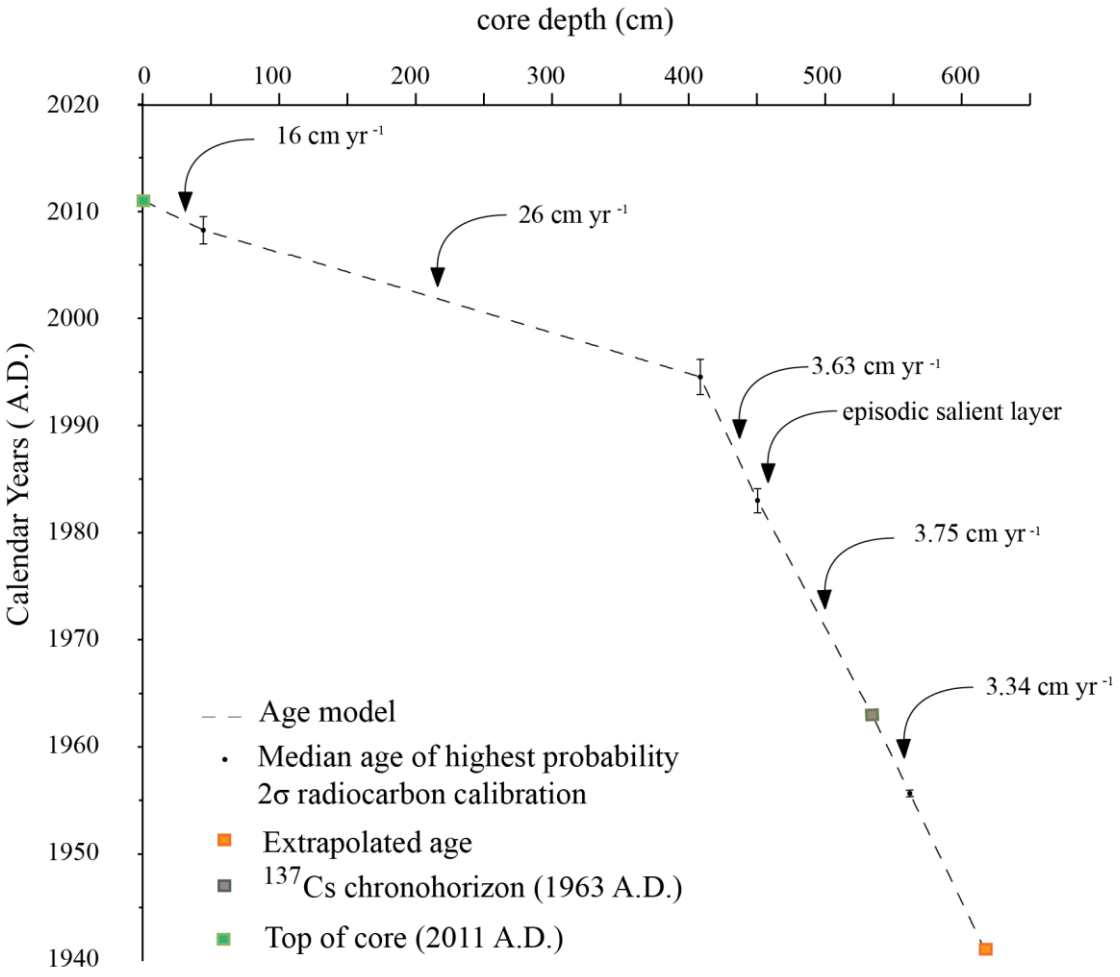

Figure 8. HCK age model and linear interpolated sedimentation rates. A distinct change in sedimentation rate occurs at 1995 CE (inflection point; see discussion). Age at base of core (~1941 CE) was determined by linear extrapolation using preceding sedimentation rate.

6. DISCUSSION

6.1 What are the differences and drivers of sedimentation and sedimentation rates in the Fillman's Creek sinkholes?

Siliciclastic and organic matter sediments are the primary sedimentary constituents in the sinkholes of Fillman's Creek observed over the time intervals sampled by the sediment cores, however, there is a single prevailing constituent in each sinkhole. In HCK visual observation of diverse organic matter throughout the core (i.e., leaves, twigs and mangrove detritus) is consistent with organic matter dominating the lithology. In comparison, siliciclastic particles dominate the sedimentary infill of SYR, with mean particle size of ~50 μm in all cores. The Fillman's Creek sinkholes also have different sedimentation rates. The sedimentation rate in Huck's Hole is remarkably high (HCK: 3.66 cm yr^{-1} to 26 cm yr^{-1}) versus the much lower sedimentation rate in Sawyer's basin (SYR: 0.5 to 47.1 mm yr^{-1}). Furthermore, both sites appear to have inconsistent sedimentation rates through time. The initial sedimentation rate at the base of HCK-D2 (3.34 cm yr^{-1}) is consistent until ~1995 CE, when sedimentation rapidly accelerates to 26 cm yr^{-1} at ~ 400 cm core depth.

The coastal location and tidal influence of the sinkholes in Fillman's Creek create vulnerability to estuarine processes. Floridian estuaries receive little sediment from rivers (Isphording et al., 1989), and they can be clogged with vegetation (i.e., the mangroves in Fillman's Creek). Based on tidal activity observed, and because no river system currently discharges into Fillman's Creek the sinkholes are in a tide dominated estuary setting (Wells, 1995). Fine sediment entering the low energy estuaries settles out, while retreating tides

move too slowly to scour away much of this deposition (Dyer, 1973). Variables impacting the volume of siliciclastic sediments transported by tidal currents in Fillman's Creek are likely tidal amplitude (affect erosion and sedimentation), overland sediment supply from erosion, and wave erosion of local sediment banks (Perillo, 1995). Tidal currents can also disrupt longshore sediment transport, and provide additional suspended sediment into micro-tidal estuaries (Davis and Fox, 1981).

The distinct features observed in the sediment records (i.e., plane and lenticular bedding) are remnants of tidal activity driving the siliciclastic deposition. The sand lenses observed (SYR: plane bedding; HCK: lenticular bedding) are common in other environments like estuaries, tidal flats, and wetlands (Perillo, 1995). Modest transport processes in Fillman's Creek (i.e., waves and tides) that transport and entrain sediment into, and out of, the estuary are likely responsible for these bedforms, however, other processes can create similar features. Small, sandy fill deposits occurring in tidal channels interspersed in black anoxic muds (Dalrymple et al., 1992) and antecedent topography (Brooks and Doyle, 1998) are two examples found to control bedding features. Because both sites have similar background sedimentation, tidal activity is likely the primary control of sand sedimentation in Fillman's Creek.

Drivers of organic matter sedimentation in the Fillman's Creek Sinkholes are different at each site. Estuaries are among the most productive of global marine ecosystems, which generate organic sedimentary particles through autochthonous production (Boynton et al., 1982; Underwood, 1999). Large quantities of river-supplied dissolved nutrients, tidal oxygen, sediment resuspension, and recirculation of nutrients and organic matter are the controlling processes that sustain the prolific phytoplankton and benthic algal production in

coastal estuaries like Fillman's Creek (Bouillon et al., 2004; Kristensen et al., 2008; Lugo and Snedaker, 1974), and drive the fine-grained, unidentifiable organic matter sedimentation observed in both sinkholes. Mangrove provide an identifiable source of organic matter in Fillman's Creek. SYR is in the upper estuary of Sawyer's Basin, considerably further from the mangroves than HCK. The identifiable mangrove detritus found exclusively in HCK is likely supplied by direct infilling from adjacent mangroves. Collins et al. (2015b) found that flooding of the epikarst surface provided a suitable environment for mangrove colonization and promoted sedimentation in adjacent karst basins. Perhaps this mechanism is the driver of sedimentation at HCK, with estuarine circulation hampering the upstream transport of larger mangrove particles to SYR. Ebb and flood tidal currents are perhaps intensifying the mangrove detritus deposition by transporting detritus from distal mangrove trees upstream to the lower estuary. However, sediment transport rates in microtidal estuaries vary with morphology, currents, and grain-size parameters (Gallivan and Davis, 1981). The sediment transport associated with tidal activity is likely responsible for the high deposition rates and organic matter infill HCK as it is closest to the estuary mouth in an area of high tidal exchange. In comparison, Sawyer's Basin is further from the estuary mouth and is subject to reduced or dissipated tidal energy. Tidal asymmetry and estuarine morphology are found to affect sediment transport or fine- and coarse-grained sediments and their associated infill in estuaries similar to Fillman's Creek (i.e., minimal or absence of river inflow) (Dronkers, 1986). Perhaps this mechanism is present in Fillman's Creek, and if so it is likely limiting the residual sediment transport upstream and into Sawyer's Basin.

6.2 How has proximity to mangroves influenced sedimentation in the two sinkholes?

Previous research has demonstrated that mangroves can impact sedimentation into coastal sinkholes and caves. In short, Collins et al. (2015a,b) documented higher sedimentation rates of organic material in submerged cave passages proximal to sinkholes that contain mangrove trees. Based on the sedimentation observed in HCK and SYR, a strong case can be made in favor of mangroves influencing sedimentation in HCK relative to SYR. Both sinkholes contain fine-grained organic matter deposition. However, two key differences between SYR and HCK are observed: the nature of the organic matter infill and the overall sedimentation rates. HCK is dominated by unconsolidated bulk organic matter and identifiable plant debris that includes mangrove propagules and leaves. In contrast, the cores from SYR were dominated by fine-grained siliciclastic material. Also, no observable plant macrofossils from mangrove trees were observed in the SYR cores. Therefore, the mangroves directly bordering the HCK sinkhole are likely impacting sedimentation in a number of ways. Litter from trees (leaves, propagules, and twigs) and subsurface root growth provide major inputs of organic carbon to mangrove sediments (Alongi, 1998), and a study by (Odum and Heald, 1972) observed remarkable detritus production in a mangrove dominated estuary from mangrove leaf-fall alone (>3 metric tons dry weight per acre per year). Additionally, mangrove sediments can effectively trap suspended material from the water column (Furukawa et al., 1997; Kitheka et al., 2002; Victor et al., 2004; Wolanski, 1995), and drive sedimentation in adjacent depositional environments like the sinkholes in Fillman's Creek.

6.3 Are hurricane signals archived as coarse-grained overwash deposits into the sinkhole, and does the stratigraphic record preserve a record of hurricane activity?

Sinkholes and blueholes are well known archives of paleo hurricane activity because elevated hydrodynamics associated with hurricane surge transport coarse-grained sediment into an otherwise quiescent pond-like environment (Denommee et al., 2014; Lane et al., 2011; van Hengstum et al., 2016). Both SYR and HCK contain obvious sand layers down core, but attributing these sand layers to only hurricane overwash processes is a challenge.

The HCK succession has numerous coarse sand layers and a massive gravel unit, but it is challenging to associate these layers to specific events (e.g., hurricane or anthropogenic event). Further confounding a direct interpretation of the sand fraction (>63 um) in the cores is the presence of the lenticular sand beds, which although they appear as an interval of elevated sand content may simply be an interval of deposition related to tidal action. At the base, both visual sand horizons and peaks in % >63 µm potentially align chronologically with historic hurricane events (i.e., 570 cm Hurricane Jeanette (cat 2)). Further upcore, however, lenticular bedding in HCK-D2 prevents confident association of sand layers with specific hurricane events. A further confounding issue is the massive gravel unit present at ~440 cm core depth. Based on the available radiocarbon dates, this feature is aged to 1983 CE. However, only 2 other intense hurricanes made landfall (< 75 nm) over the time interval sampled by the HCK core (i.e., Hurricanes Donna in 1960 CE and Easy in 1953 CE; category 3), and neither event deposited such a salient gravel layer as was deposited in 1983, when no intense

hurricane event made landfall near Fillman's Creek. It is possible that several of the coarse sand layers that clearly extend across the core sample from HCK are hurricane events and not lenticular sand beds, but the presence of the lenticular sand bends in HCK introduces uncertainty in interpreting the drivers of sand deposition into Huck's Hole. Furthermore, if the high sedimentation rates observed in HCK-D2 are indicative of long-term sedimentation rates at HCK, significantly longer sediment cores will be required to assess possible sedimentation at Huck's Hole on millennial timescales.

Coarse-grained deposits also occur in all SYR cores. Visual identification and particle size analysis confirm the most prominent coarse-grained horizon occurs at similar depths across all 3 cores, such as at 64 cm in SYR-D1, 71 cm in SYR-D3, and 71 cm in SYR-D4. Chronological control gives support that both SYR-D1 and SYR-D3 have indeed captured the same deposition, though no aging was applied to SYR-D4 and therefore stating the same coarse-grained horizon as captured in SYR-D4 is purely speculative. Because the sedimentation rate in SYR was less than HCK over the historical period, identification of specific hurricane events for historical calibration of the sediment record was problematic. It is possible that these coarse-grained horizons do correspond to previous hurricane events, but robust hurricane reconstructions require adequate control of the drivers of historic event beds in the stratigraphic record. Given the limitations for dating material in SYR and evidence for changes in sedimentation rate, SYR may not be the best location for reconstructing paleo hurricane activity for the western coast of Florida.

6.4 Has coastal urbanization impacted sedimentation rates in the sinkholes?

The watershed and coastal landscape adjacent to Fillman's Creek has been modified by anthropogenic activity through time. Based on aerial photographs, the onset of coastal modification likely began after 1941 CE, as the aerial photograph from this time depicts little anthropogenic modification around Fillman's Creek (Fig. 2). By 1957 CE, a roadway and culvert divides the upper part of the estuary from the lower part. Neither an immediate impact, nor a delayed impact to the sedimentation rate in either sinkhole in Fillman's Creek is discernable in the sediment cores, based on the available data. Problematically, the low sedimentation rate in SYR over the last 50 years makes discerning the impacts of this event (i.e., culvert installation) a challenge. Perhaps this event is the cause for the low sedimentation rates observed in SYR, but this possibility is speculative without better age control in the SYR successions. In contrast, a higher-resolution sedimentation rate is available from HCK that could have documented sedimentary changes from anthropogenic activity in the watershed. The two most prominent features are the change in sedimentation rate at 1995 CS (3.63 cm yr^{-1} to 26 cm $yr^{-1)}$, and the prominent coarse-grained horizon at 460 cm deep in the core that is likely aged to ~1982 CE. It is likely that the most significant stressors to the local sedimentary régime are installation of the large coastal community by 1971 CE (Fig. 2C), installation of the culvert through Fillman's Creek (1957 CE), or increased structures on the adjacent watershed (e.g., roads or buildings). Perhaps one would hypothesize that watershed urbanization reduced land surface vegetation, thus elevating surface runoff, and lead to increased sedimentation into the sinkholes in Fillman's

Creek. However, these salient sedimentary features that are observed in HCK (i.e., gravel horizon, change in sedimentation rate) considerably post-date these potential stressors to the local sedimentary régime.

Erosion of the local landscape can be complex in areas with urbanization and coastal development. A coastal community is emplaced directly north and adjacent to the mouth of Fillman's Creek, and a study by Dellapenna et al. (2015) found similar anthropogenic influence including the substitution of mangrove-forested shorelines with concrete bulkheads and installation of residential canals had both directly and indirectly shifted sediment distributions significantly in the local estuarine system. It is plausible that canalization in the watershed has diverted regional hydrogeologic flow pathways in the limestone bedrock, such that Fillman's Creek now has decreased discharge in compared to its original natural state. This may partially explain both the increased (decrease) in sedimentation rate at HCK (SYR), but resolving this uncertainty requires higher-resolution age models.

However, sedimentation rate is not the only way to detect urbanization. Activities associated with urbanization are likely to impact coastal wetlands by altering their hydrological regimes, water quality, organic matter and nutrient sources in addition to sedimentation (Faulkner, 2004). Studies in the past have attempted identification of urbanization impact in a piecemeal matter, but ultimately an ecosystem approach may be best to identify effects of urbanization on estuarine sedimentation (Lee et al., 2006). A strong case for using sinkhole sediments as baseline data on wetland (or estuary) ecosystem dynamics is sinkholes provide undisturbed depositional sites that may allow

temporal study of potential ecosystem stress. Perhaps additional chemical and biological analyses of HCK and SYR may further inform impacts of urbanization.

7. CONCLUSIONS

Previous studies indicate sediment archives in sinkholes and blueholes in both Cenozoic and Mesozoic carbonate platforms preserve important records of paleoenvironmental change. As such this study focused on three objectives: first, to identify the primary sedimentary constituents and sedimentation rates in submerged sinkholes in west central Florida, second, to evaluate if sinkhole sedimentation is susceptible to impacts from coastal modification, and third, to evaluate the suitability of sinkhole successions in west central Florida to credit paleo hurricane research. Overall, siliciclastic mud and organic matter sediments are the primary sedimentary constituents in the sinkholes of Fillman's Creek. The sinkhole closest to the estuary mouth with more mangrove trees (HCK) did will have higher organic matter deposition and sedimentation rate, which is consistent with other studies demonstrating the important of mangrove environments influencing sedimentation in karst basin (Collins et al., 2015b). Based on the results generated during this study, the impacts of watershed urbanization on sedimentation patterns within the Fillman's Creek sinkholes was not detected. But, that does not mean that there was no impact. Longer sediment cores with more robust age-modeling and additional data from erosion of overland sediment supply and surface water runoff from nearby watersheds would be required to completely resolve sedimentation patterns in Fillman's Creek.

Reconstructing paleo hurricane activity in these sites was hampered by\ high sedimentation rates and flaser sediment beds in HCK, and a lack of suitable material to

build a robust age model in SYR (i.e., terrestrial plant macrofossils). To better understand paleo hurricane activity on the western coast of Florida using sinkhole sediments, the results of this study suggest that it may be better to investigate sinkholes outside of micro-tidal estuaries with urbanized watersheds. In such localities, the drivers of sinkhole sedimentation patterns may prove easier to relate to hurricane-mediated processes on modern and paleo timescales.

REFERENCES

Aerial Park Survey, I., 1974. Pasco County, Florida, in: Service, A.S.a.C. (Ed.). U.S. Department of Agriculture, University of Florida Map and Digital Imagery Library.

Alongi, D.M., 1998. Coastal ecosystem processes. CRC Press, Boca Raton. 14-22.

Baumann, R.H., Day, J.W., Miller, C.A., 1984. Mississippi deltaic wetland survival: sedimentation versus coastal submergence. Science 224, 1093-1095.

Bouillon, S., Moens, T., Overmeer, I., Koedam, N., Dehairs, F., 2004. Resource utilization patterns of epifauna from mangrove forests with contrasting inputs of local versus imported organic matter. Marine ecology-progress series 278, 77-88.

Boynton, W., Kemp, W., Keefe, C., 1982. A comparative analysis of nutrients and other factors influencing estuarine phytoplankton production. United States Department of Energy Office of Health and Environmental Research.

Brinkmann, R., Reeder, P., 1994. The influence of sea-level change and geologic structure on cave development in west-central Florida. Physical Geography 15, 52-61.

Brooks, G.R., Doyle, L.J., 1998. Recent sedimentary development of Tampa Bay, Florida: a microtidal estuary incised into Tertiary platform carbonates. Estuaries 21, 391-406.

Budd, D.A., 2001. Permeability loss with depth in the Cenozoic carbonate platform of west-central Florida. AAPG bulletin 85, 1253-1272.

Callaway, J.C., Zedler, J.B., 2004. Restoration of urban salt marshes: lessons from southern California. Urban Ecosystems 7, 107-124.

Collins, S., Reinhardt, E., Werner, C., Le Maillot, C., Devos, F., Meacham, S., 2015a. Regional response of the coastal aquifer to Hurricane Ingrid and sedimentation

flux in the Yax Chen cave system (Ox Bel Ha) Yucatan, Mexico. Palaeogeography, Palaeoclimatology, Palaeoecology 438, 226-238.

Collins, S., Reinhardt, E., Werner, C., Le Maillot, C., Devos, F., Rissolo, D., 2015b. Late Holocene mangrove development and onset of sedimentation in the Yax Chen cave system (Ox Bel Ha) Yucatan, Mexico: Implications for using cave sediments as a sea-level indicator. Palaeogeography, Palaeoclimatology, Palaeoecology 438, 124-134.

Culter, J., 2006. Exploration of the West Florida Shelf Blue Holes Investigation of Physical and Biological Characteristics and Archaeological Implications of Unique Karst Features, AGU Fall Meeting Abstracts, p. 08.

Dalrymple, R.W., Zaitlin, B.A., Boyd, R., 1992. Estuarine facies models: conceptual basis and stratigraphic implications: perspective. Journal of Sedimentary Petrology 62, 1130-1146.

Davis Jr, R., Fitzgerald, D., 2009. Beaches and coasts. John Wiley & Sons, Malden, MA.

Davis, R.A., Fox, W.T., 1981. Interaction between wave-and tide-generated processes at the mouth of a microtidal estuary: Matanzas River, Florida (USA). Marine Geology 40, 49-68.

Dellapenna, T.M., Fielder, B., Noll IV, C.J., Savarese, M., 2015. Geological responses to urbanization of the Naples Bay estuarine system, Southwestern Florida, USA. Estuaries and Coasts 38, 81-96.

Denommee, K., Bentley, S., Droxler, A., 2014. Climatic controls on hurricane patterns: a 1200-y near-annual record from Lighthouse Reef, Belize. Scientific reports 4.

Dronkers, J., 1986. Tidal asymmetry and estuarine morphology. Netherlands Journal of Sea Research 20, 117-131.

Dyer, K.R., 1973. Estuaries: a physical introduction. John Wiley & Sons, Londen. 44-50.

Faulkner, S., 2004. Urbanization impacts on the structure and function of forested wetlands. Urban Ecosystems 7, 89-106.

Florea, L.J., 2006. Architecture of air-filled caves within the karst of the Brooksville Ridge, west-central Florida. Journal of Cave and Karst Studies 68, 64-75.

Florea, L.J., Budd, D.A., Brinkman, R.B., 2009. Caves and karst of west-central Florida. Geography/Geology Faculty Publications, 21.

Furukawa, K., Wolanski, E., Mueller, H., 1997. Currents and sediment transport in mangrove forests. Estuarine, Coastal and Shelf Science 44, 301-310.

Gallivan, L.B., Davis, R.A., 1981. Sediment transport in a microtidal estuary: Matanzas River, Florida (USA). Marine Geology 40, 69-83.

Garman, K.M., Garey, J.R., 2005. The transition of a freshwater karst aquifer to an anoxic marine system. Estuaries 28, 686-693.

Gischler, E., Shinn, E.A., Oschmann, W., Fiebig, J., Buster, N.A., 2008. A 1500-year Holocene Caribbean climate archive from the Blue Hole, Lighthouse reef, Belize. Journal of Coastal Research, 1495-1505.

Grimm, E.C., Jacobson, G., Watts, W.A., Hansen, B.C., Maasch, K.A., 1993. A 50,000-year record of climate oscillations from florida and its temporal correlation. Science 261, 198-200.

Gulley, J., Martin, J., Moore, P., Murphy, J., 2013. Formation of phreatic caves in an eogenetic karst aquifer by CO2 enrichment at lower water tables and subsequent flooding by sea level rise. Earth Surface Processes and Landforms 38, 1210-1224.

Gulley, J., Martin, J., Spellman, P., Moore, P., Screaton, E., 2014. Influence of partial confinement and Holocene river formation on groundwater flow and dissolution in the Florida carbonate platform. Hydrological Processes 28, 705-717.

Horner, R.R.C., Sarah S.; Reinelt, Lorin E.; Ludwa, Kenneth A.; Chin, Nancy T.; Valentine, Marian, 2000. Wetlands and urbanization: Implications for the future. Lewis Publishers, Boca Raton.

Isphording, W.C., Imsand, F.D., Flowers, G.C., 1989. Physical characteristics and aging of Gulf Coast estuaries. Gulf Coast Association of Geological Societies Transactions 39, 387-401.

Jansa, L., 1981. Mesozoic carbonate platforms and banks of the eastern North American margin. Marine Geology 44, 97-117.

Kitheka, J.U., Ongwenyi, G.S., Mavuti, K.M., 2002. Dynamics of suspended sediment exchange and transport in a degraded mangrove creek in Kenya. AMBIO: A Journal of the Human Environment 31, 580-587.

Kjellmark, E., 1996. Late Holocene climate change and human disturbance on Andros Island, Bahamas. Journal of Paleolimnology 15, 133-145.

Kovacs, S.E., van Hengstum, P.J., Reinhardt, E.G., Donnelly, J.P., Albury, N.A., 2013. Late Holocene sedimentation and hydrologic development in a shallow coastal sinkhole on Great Abaco Island, The Bahamas. Quaternary International 317, 118-132.

Kristensen, E., Bouillon, S., Dittmar, T., Marchand, C., 2008. Organic carbon dynamics in mangrove ecosystems: a review. Aquatic Botany 89, 201-219.

Land, L., Paull, C., 2000. Submarine karst belt rimming the continental slope in the Straits of Florida. Geo-Marine Letters 20, 123-132.

Lane, P., Donnelly, J.P., Woodruff, J.D., Hawkes, A.D., 2011. A decadally-resolved paleohurricane record archived in the late Holocene sediments of a Florida sinkhole. Marine Geology 287, 14-30.

Lee, S.Y., Dunn, R.J.K., Young, R.A., Connolly, R.M., Dale, P., Dehayr, R., Lemckert, C.J., McKinnon, S., Powell, B., Teasdale, P., 2006. Impact of urbanization on coastal wetland structure and function. Austral Ecology 31, 149-163.

Lugo, A.E., Snedaker, S.C., 1974. The ecology of mangroves. Annual review of ecology and systematics, 39-64.

Menning, D.M., Wynn, J.G., Garey, J.R., 2015. Karst estuaries are governed by interactions between inland hydrological conditions and sea level. Journal of Hydrology 527, 718-733.

Milliken, K., Anderson, J.B., Rodriguez, A.B., 2008. A new composite Holocene sea-level curve for the northern Gulf of Mexico, in: Anderson, J.B.R., A.B. (Ed.), Response of Upper Gulf Coast Estuaries to Holocene Climate Change and Sea-Level Rise: Geological Society of America Special Paper 443. The Geological Society of America, pp. 1-11.

Mylroie, J.E., Carew, J.L., Vacher, H., 1995. Karst development in the Bahamas and Bermuda, in: Curran, A.H.W., B. (Ed.), Terrestrial and shallow marine geology of the Bahamas and Bermuda. Geological Society of America, Boulder, Colorado, pp. 251-268.

Mylroie, J.E., Mylroie, J.R., 2013. Caves and karst of the Bahama Islands, Coastal Karst Landforms. Springer, pp. 147-176.

Mylroie, J.E., Panuska, B.C., Carew, J.L., Frank, E.F., Taggart, B.E., Troester, J.W., Carrasquillo, R., 1995b. Development of flank margin caves on San Salvador Island, Bahamas and Isla de Mona, Puerto Rico. Bahamian Field Station.

Mylroie, J.E.M., Joan R., 2013. Coastal karst development in carbonate rocks, in: Lace, M.L.M., John E. (Ed.), Coastal Karst Landforms. Springer, Dordrecht, pp. 77-109.

NOAA, T.a.C., 2015. New Port Richey, Pithlachascotee River, FL StationId:8727001, Referenced to Station: CEDAR KEY (8727520). NOAA / National Ocean Service, Center for Operational Oceanic Products and Services, p. 1p.

Odum, W.E., Heald, E.J., 1972. Trophic analyses of an estuarine mangrove community. Bulletin of Marine Science 22, 671-738.

Pennington, W., Tutin, T., Cambray, R., Fisher, E., 1973. Observations on lake sediments using fallout 137Cs as a tracer. Nature 242, 324-326.

Perillo, G.M., 1995. Geomorphology and sedimentology of estuaries: An introduction, in: Perillo, G.M. (Ed.), Geomorphology and Sedimentology of Estuaries, 53 ed. Elsevier, Amsterdam, The Netherlands, pp. 1-16.

Puri, H.S., 1957. Stratigraphy and zonation of the Ocala Group. Florida Geological Survey.

Randazzo, A.F., Kosters, M., Jones, D.S., Portell, R.W., 1990. Paleoecology of shallow-marine carbonate environments, middle Eocene of Peninsular Florida. Sedimentary Geology 66, 1-11.

Reed, D.J., 1989. Patterns of sediment deposition in subsiding coastal salt marshes, Terrebonne Bay, Louisiana: the role of winter storms. Estuaries 12, 222-227.

Rejmanek, M., Sasser, C.E., Peterson, G.W., 1988. Hurricane-induced sediment deposition in a Gulf coast marsh. Estuarine, Coastal and Shelf Science 27, 217-222.

Ritchie, J.C., McHenry, J.R., 1990. Application of radioactive fallout cesium-137 for measuring soil erosion and sediment accumulation rates and patterns: a review. Journal of Environmental Quality 19, 215-233.

Schmitter-Soto, J.J., Arce-Ibarra, A.M., Vásquez-Yeomans, L., 2002. Records of Megalops atlanticus in the Mexican Caribbean coast. Contribributions in Marine Science 35, 34-42.

Schoellhamer, D.H., 1995. Sediment resuspension mechanisms in old Tampa Bay, Florida. Estuarine, Coastal and Shelf Science 40, 603-620.

Scott, T.M., Anderson, D., 2001. Geologic map of the State of Florida. Florida Geological Survey.

Shinn, E.A., Reich, C.D., Locker, S.D., Hine, A.C., 1996. A giant sediment trap in the Florida Keys. Journal of Coastal Research 12, 953-959.

Slayton, I.A., 2010. A vegetation history from Emerald Pond, Great Abaco Island, the Bahamas, based on pollen analysis. University of Tennessee, Knoxville.

Stevenson, J., Ward, L., Kearney, M., 1986. Vertical accretion in marshes with varying rates of sea level rise, in: Wolfe, T.A. (Ed.), Estuarine Variability. Academic Press, Orlando, FL, pp. 241-259.

Surveys, R.A., 1957. Pasco County, Florida, in: Service, C.S. (Ed.). U.S. Department of Agriculture, University of Florida Map and Digital Imagery Library.

Swarzenski, P., Reich, C., Spechler, R., Kindinger, J., Moore, W., 2001. Using multiple geochemical tracers to characterize the hydrogeology of the submarine spring off Crescent Beach, Florida. Chemical Geology 179, 187-202.

Teeter, J.W., Quick, T.J., 1990. Magnesium-salinity relation in the saline lake ostracode *Cyprideis americana*. Geology 18, 220-222.

Underwood, G.J.C.K., J., 1999. Primary Production by Phytoplankton and Microphytobenthos in Estuaries, in: Nedwell, N.B.R., D.G. (Ed.), Advances in Ecological Research. Academic Press, London, pp. 93-139.

van Hengstum, P.J., Donnelly, J.P., Fall, P.L., Toomey, M.R., Albury, N.A., Kakuk, B., 2016. The intertropical convergence zone modulates intense hurricane strikes on the western North Atlantic margin. Scientific reports 6.

van Hengstum, P.J., Donnelly, J.P., Toomey, M.R., Albury, N.A., Lane, P., Kakuk, B., 2013. Heightened hurricane activity on the Little Bahama Bank from 1350 to 1650 AD. Continental Shelf Research 86, 103-115.

van Hengstum, P.J., Reinhardt, E.G., Beddows, P.A., Gabriel, J.J., 2010. Linkages between Holocene paleoclimate and paleohydrogeology preserved in a Yucatan underwater cave. Quaternary Science Reviews 29, 2788-2798.

van Hengstum, P.J., Scott, D.B., Gröcke, D.R., Charette, M.A., 2011. Sea level controls sedimentation and environments in coastal caves and sinkholes. Marine Geology 286, 35-50.

Victor, S., Golbuu, Y., Wolanski, E., Richmond, R., 2004. Fine sediment trapping in two mangrove-fringed estuaries exposed to contrasting land-use intensity, Palau, Micronesia. Wetlands Ecology and Management 12, 277-283.

Watts, W., Hansen, B., Grimm, E., 1992. Camel Lake: a 40 000-yr record of vegetational and forest history from northwest Florida. Ecology, 1056-1066.

Wells, J.T., 1995. Tide-dominated estuaries and tidal rivers. Developments in Sedimentology 53, 179-205.

Winkler, T.S., van Hengstum, P.J., Horgan, M.C., Donnelly, J.P., Reibenspies, J.H., 2016. Detrital cave sediments record Late Quaternary hydrologic and climatic variability in northwestern Florida, USA. Sedimentary Geology 335, 51-65.

Wolanski, E., 1995. Transport of sediment in mangrove swamps. Hydrobiologia 295, 31-42.

Zarikian, C.A.A., Swart, P.K., Gifford, J.A., Blackwelder, P.L., 2005. Holocene paleohydrology of Little Salt Spring, Florida, based on ostracod assemblages and stable isotopes. Palaeogeography, Palaeoclimatology, Palaeoecology 225, 134-156.